Numerical Study of Circular Hydraulic Jump Using Volume-of-Fluid Method

Mohammad Passandideh-Fard
Associate Professor
e-mail: mpfard@um.ac.ir

Ali Reza Teymourtash
Assistant Professor
e-mail: teymourtash@um.ac.ir

Mohammad Khavari
e-mail: mohammad.khavari@yahoo.com

Department of Mechanical Engineering,
Ferdowsi University of Mashhad,
Azadi Square,
9177948944 Mashhad, Iran

When a vertical liquid jet impacts on a solid and horizontal surface, the liquid starts spreading radially on the surface, until a sudden increase in the fluid height occurs and a circular hydraulic jump (CHJ), easily seen in the kitchen sink, is formed. In this study, the formation of CHJ is numerically simulated by solving the flow governing equations, continuity and momentum equations, along with an equation to track the free surface advection using the volume-of-fluid (VOF) method and Youngs' algorithm. The numerical model is found to be capable of simulating the jump formation and its different types. Extensive comparisons are performed between the model results and those of the available experiments and modified Watson's theory. The model is shown to accurately predict the jump location and its behavior. Also a parametric study for the effects of different parameters including volumetric flow rate, downstream height, viscosity and gravity on the jump radius, and its characteristics is carried out. Compared with previous works on CHJ available in the literature, employing the VOF method considering the surface tension effects and performing a full parametric study and a complete comparison with experiments and theory are new in this paper. The simulations are performed for two different liquids, water and ethylene glycol, where it is found that the jump is more stable and its location is less sensitive to the downstream height for the more viscous liquid (ethylene glycol). When the downstream height is increased, the radius of the circular hydraulic jump reduces up to a certain limit after which there would be no stable jump. If the gravity is decreased, the radius of the jump and the length of the transition zone will both increase. The radius of the jump in microgravity conditions is less sensitive to the downstream height than it is in normal gravity. [DOI: 10.1115/1.4003307]

Keywords: liquid jet impingement, circular hydraulic jump, numerical flow simulation, volume-of-fluid method

1 Introduction

At the beginning of the 20th century, the great British physicist, Lord Rayleigh encountered a discontinuity in the geometry of linear one-dimensional flow. The structure is called *river bore* if moving and *hydraulic jump* if stationary and is created due to, for example, variation in river bed. The classical planar hydraulic jump, which occurs in open-channel flows, is a very old and well-known phenomenon thoroughly considered in the literature. However, the circular hydraulic jump (CHJ) although having a similar name, is completely a different phenomenon. When a circular vertical liquid jet impacts on a solid horizontal surface, which is called *target plate*, the flow spreads radially away everywhere—from the stagnation point—until at a particular radius, which is called the radius of the jump, the thickness of the liquid film increases abruptly and a so-called circular or axisymmetric hydraulic jump occurs. The impingement of the circular jet on the solid surface is important in a variety of processes such as the fuel tank of space shuttles, aircraft generator coils, coating flows, impingement cooling of electronic devices, laser mirrors, and material processing in manufacturing [1]. The important feature of the CHJ is its potential for the heat loss in the downstream of the jump, especially for the processes in which the purpose is cooling a hot surface, such as the research done by Womac et al. [2].

The first person who considered hydraulic jump was probably Lord Rayleigh [3] who proposed his model by using the continuity and momentum equations and assuming the flow to be inviscid. He assumed that mass and momentum are conserved across the jump, but energy is not (some energy is lost across the jump due to the viscous dissipation related to the flow recirculation at the jump). He finally could derive some relations for the inviscid jump. Rayleigh's method was based on the analogy of shallow water and gas theories. The complete theory of inviscid circular hydraulic jump was presented by Birkhoff and Zarantonello [4].

However, because of the thinness of the fluid layer, particularly before the jump, it is clear that the flow in such a problem is viscous and the inviscid theory is not adequate for predicting the location of the circular hydraulic jump. Therefore, the viscosity must be taken into account. The first who considered the effect of viscosity on CHJ was Watson [5], who solved the problem analytically. He described the flow in terms of a Blasius sublayer developing in the vicinity of the stagnation point, as on a flat plate, and also in terms of a similarity solution. By using the momentum equation, he could finally obtain a relation for predicting the radius of the jump assuming the downstream height to be known. Watson's model will be considered in detail in Sec. 2.

There were also some earlier works on CHJ done by Tani [6] and Kurihara [7] who, unaware of each other's work, obtained the same result that was later known as the Tani–Kurihara theory. In their theory, the source of the circular hydraulic jump is assumed to be the separation of the flow and the formation of a vortex on the wall below the jump.

The validity of Watson's theory has been investigated experimentally by many different researchers throughout the world in the last four decades such as Watson himself [5], Olson and Turkdogan [8], Ishigai et al. [9], Nakoryakov et al. [10], Bouhadef [11], Craik et al. [12], Errico [13], Vasista [14], Liu and Lienhard

Contributed by the Fluids Engineering Division of ASME for publication in the JOURNAL OF FLUIDS ENGINEERING. Manuscript received May 8, 2010; final manuscript received December 11, 2010; published online January 28, 2011. Assoc. Editor: Dimitris Drikakis.

[15], Ellegaard et al. [16], and in particular Bush and Aristoff [17,18]. The agreement between the theory and experiments has been diverse depending on the jump conditions.

Bowles and Smith [19] studied the circular hydraulic jump—with surface tension considerations—and the small standing waves preceding the jump. Higuera [20] also proposed a model for planar jump by studying the flow in transition region in the limit of infinite Reynolds number. Bohr et al. [21] applied the shallow-water theory to the CHJ and obtained a scaling relation for the jump radius. Later, they also proposed a simple viscous theory for free-surface flows that can accommodate regions of separated flow and yield the structure of stationary hydraulic jumps [22].

Watanabe et al. [23] presented integral methods for shallow free-surface flows with separation in the application of circular hydraulic jump and also the flow down an inclined plane. Ellegaard et al. who had already investigated the CHJ empirically [16], for the very first time, observed the polygonal hydraulic jumps in their experiments [24] and reported them in detail later [25]. In the same year, Yokoi and Xiao [26] considered the transition in the circular hydraulic jump numerically. Three years later, they also studied numerically the structure formation in circular hydraulic jumps with moderate Reynolds numbers [27]. Brechet and Neda [28] also investigated the circular hydraulic jumps and compared their theory with experiments.

Avedisian and Zhao [1] studied in detail the effect of gravity on the circular hydraulic jump experimentally. They showed that reducing the gravity will make the jump radius larger and its curvature smaller. According to their observations, in low gravity conditions, the radius of the jump is higher than that of the normal gravity conditions. The length of the transition zone was also found to be larger, i.e., the jump occurs more gradually. They also observed that the jump radius is almost *independent* of the downstream height in low gravity conditions, while as many researchers have shown, this height is a vital parameter in normal gravity conditions. They found that the effect of surface tension and viscosity was dominant at low gravity conditions [1].

Rao and Arakeri [29] considered the CHJ empirically and measured the radius of the jump, film thickness, and the length of the transition zone; they specially focused on jump formation and transition to turbulent flow. Ferreira et al. [30] simulated the circular hydraulic jump numerically in order to compare the various upwind schemes for convective term of the Navier–Stokes equations. However, the effect of surface tension in their numerical model has not been considered.

Gradeck et al. [31] studied the impingement of an axisymmetric jet on a moving surface both numerically and experimentally in order to simulate the cooling of a rolling process in the steel making industry. Ray and Bhattacharjee [32] also studied the standing and traveling waves in the CHJ. Very recently, Mikielewicz and Mikielewicz [33] proposed a simple dissipation model for the CHJ. Kate et al. [34] studied experimentally the impingement of an oblique liquid jet on a solid surface causing a noncircular jump. They also measured the film thickness and the stagnation pressure for different angles of the incoming jet. Kasimov [35] continued the work done by Tani [6], Kurihara [7], and Bohr et al. [21] to obtain relations for predicting the jump radius and the film thickness upstream and downstream of the jump; he compared the circular hydraulic jump with the detonation wave in gasdynamics. The imperfections of the theory of Bohr et al. [21] such as lack of asymptotic solutions and also blowing up the solutions at a particular radius (radius of the disk) did not exist in the Kasimov theory. Middleman [36] presented a complete review of the circular hydraulic jump and described the phenomenon in nondimensional form.

In this study, the impingement of a vertical liquid jet on a solid surface is simulated employing an in-house code developed based on the method of volume-of-fluid (VOF) using Youngs' algorithm for the advection of the free surface. As stated earlier, many numerical works on CHJ available in the literature did not consider the effect of surface tension; in this study, however, this effect has been considered using the continuum surface force (CSF) model. The model is validated by a full comparison between the results of simulations with those of the available experiments and theory. The model is shown to be capable of simulating different types of the CHJ as well. The effects of different parameters such as downstream height, volumetric flow rate, and gravity are also investigated in detail. The main contribution of this paper compared with the previous works can be stated to be the use of the VOF method considering the surface tension effects, the investigation of the effects of important parameters, and the presentation of a complete comparison with both experiments and theory.

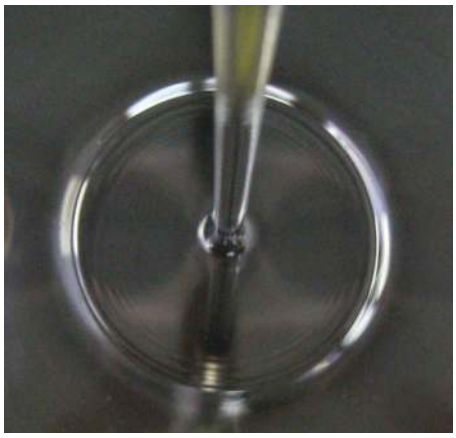

Fig. 1 The circular hydraulic jump [45]

2 Theory of Circular Hydraulic Jump

In this section, the viscous theory of a circular hydraulic jump proposed by Watson [5] and later modified by Bush and Aristoff [17]—by introducing the effect of surface tension—is briefly discussed. Upon impact of a vertical liquid jet on a solid surface, a circular hydraulic jump may occur; a sample of an empirically observed CHJ is shown in Fig. 1. For further elaboration of the phenomenon, the general structure of CHJ is also shown in Fig. 2.

As mentioned in the Introduction, Watson was the first person who analyzed the viscous circular hydraulic jump. He used the boundary layer theory for the upstream of the jump and assumed the flow in the downstream region to be inviscid. Assuming the pressure thrust to be equal to the rate of momentum destruction, he derived the following for the jump condition:

$$\frac{1}{2}g(H_\infty^2 - H^2) = \left(\frac{Q}{2\pi R_j}\right)^2 \left(\frac{1}{H} - \frac{1}{H_\infty}\right) \tag{1}$$

where H is the upstream height, H_∞ the downstream height (or outer depth), g the gravitational acceleration, Q the volumetric flow rate, and R_j is the radius of the jump. The final result of the inviscid theory in nondimensional form, obtained by neglecting the term containing $(H/H_\infty)^2$ in Eq. (1) and making some substitutions, is given by

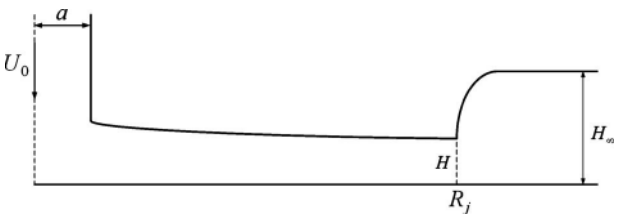

Fig. 2 The general structure of circular hydraulic jump

$$\frac{R_j H_\infty^2 g a^2}{Q^2} + \frac{a^2}{2\pi^2 R_j H_\infty} = \frac{1}{\pi^2} \tag{2}$$

where a is the radius of the incoming jet before impact. Watson showed that the inviscid theory is not accurate enough for predicting the radius of the jump by comparing his experimental results with this theory. The same conclusion is made from numerical results, as discussed later in this paper.

In order to derive his viscous theory, Watson ignored the hydrostatic pressure and obtained a similarity solution for the problem. He argued that upon impact of a liquid jet on the surface, the boundary layer would grow from the stagnation point until it engulfs the flow entirely. Thus, he divided the upstream flow into four different regions: the region $r=O(a)$ very close to the point of impact; the region $r \gg a$ in which the boundary layer is similar to that of Blasius over flat plate; a small transition region; and finally the region in which the flow is completely unaffected by the original flow, and the similarity solution suggested by Watson is valid. Ignoring the third region and applying the method of Karman–Pohlhausen to match the Blasius layer in the second region along with his own similarity solution in the forth region, Watson proposed following velocity profile:

$$u = U(r) f\left(\frac{z}{\delta}\right) \tag{3}$$

where $U(r)$ is the surface velocity, δ is the boundary layer thickness, and f is the similarity function. He introduced a defining radius of $r=r_0$ across which the properties of the flow change significantly. For $r<r_0$, the velocity profile is similar to that of Blasius over a flat plate, the boundary layer thickness is $\delta<H$, and the surface velocity is $U(r)=U_0$. At $r=r_0$, the boundary layer reaches the free surface and captures the whole flow. For $r>r_0$, the velocity profile is of the type of similarity solution obtained by Watson, Eq. (3) with $\delta=H$. The value of the defining radius (r_0) is obtained by the condition $\delta=H$, which eventually leads to $r_0 = 0.3155a\,\mathrm{Re}^{1/3}$ [5].

Watson assumed the flow to be laminar and ignored the effect of surface tension and hydrostatic pressure in his analysis. Bush and Aristoff [17] studied the CHJ both experimentally and analytically in which they considered the influence of surface tension. By proposing a simple relation for the curvature force—which for weak jumps is comparable to pressure forces in momentum equation—they modified Watson's theory as [17]

$$\frac{R_j H_\infty^2 g a^2}{Q^2}\left(1 + \frac{2}{Bo}\right) + \frac{a^2}{2\pi^2 R_j H_\infty} = 0.10132 - 0.1297\left(\frac{R_j}{a}\right)^{3/2} \mathrm{Re}^{-1/2} \quad r < r_0 \tag{4}$$

$$\frac{R_j H_\infty^2 g a^2}{Q^2}\left(1 + \frac{2}{\mathrm{Bo}}\right) + \frac{a^2}{2\pi^2 R_j H_\infty} = 0.01676\left[\left(\frac{R_j}{a}\right)^3 \mathrm{Re}^{-1} + 0.1826\right]^{-1} \quad r \geq r_0 \tag{5}$$

where $\mathrm{Bo}=\rho g R_j \Delta H/\sigma$ is the Bond number, $\mathrm{Re}=Q/\upsilon a$ is the Reynolds number, ρ is the density, υ is the kinematic viscosity, σ is the surface tension, and ΔH is the jump height.

The above relations for the jump radius differ from those of Watson [5] only in the term including Bond number that contains the surface tension effect, which is highlighted in the weak jump regimes. By this modification to Watson's theory, Bush and Aristoff [17] could improve the accuracy of his model in small jump regimes in which his own theory had some imperfections. According to the above relations, for the strong jumps with large radius, the Bond number will be large; as a result, its effect on the above equations will become negligible and Watson's theory will be recovered.

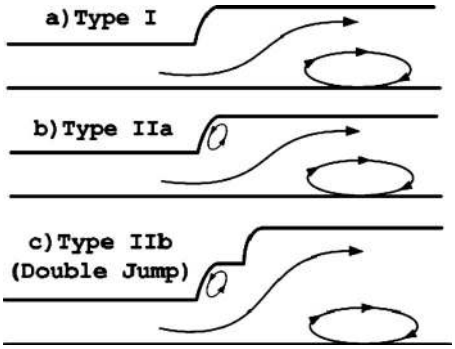

Fig. 3 Schematics of different types of circular hydraulic jump as introduced by Bush et al. [18]

Using a shallow-water approach, Bohr et al. [21] presented a scaling relation for the circular hydraulic jump radius as

$$R_j \sim q^{5/8} \upsilon^{-3/8} g^{-1/8} \tag{6}$$

where $q=Q/(2\pi)$ and R_j is the radius of the jump. According to this relation, decreasing gravity and viscosity and also increasing the flow rate will result in larger jumps. They verified the validity of this power law relation using their measurements [21] and the experimental results of Tani [6]. As shown later in this paper, the same flow characteristics are also seen from the numerical results (see Figs. 11 and 12).

Based on different features observed experimentally, Bush et al. [18] classified the CHJ into two types. According to their classification, the type I jump, as shown schematically in Fig. 3(*a*), is the standard CHJ in which the surface flow is radially outward everywhere and is also marked by the separation of the boundary layer below the jump and on the surface. Increasing the downstream height changes the jump structure classified into type IIa and IIb by Bush et al. [18]. The type IIa jump, shown in Fig. 3(*b*), is marked by a separation bubble on the wall and also by a region of reversed flow (also known as *surface roller*) at the jump front. In this type of jump, the main stream flows between these two vortices. If the downstream height is increased further, the jump will transform to type IIb also called *double jump* in which the thickness of the fluid layer increases twice as shown schematically in Fig. 3(*c*). The above classification of CHJ reveals the importance of the downstream height in the flow structure, which will be studied later in this paper.

3 Numerical Method

In this study, the circular hydraulic jump is simulated numerically by solving the Navier–Stokes equations, along with an equation for tracking the free-surface. In this section, a brief account of the numerical method is presented. The governing equations are the continuity and momentum equations

$$\nabla \cdot \mathbf{V} = 0 \tag{7}$$

$$\frac{\partial \mathbf{V}}{\partial t} + \nabla \cdot (\mathbf{V}\mathbf{V}) = -\frac{1}{\rho}\nabla p + \frac{1}{\rho}\nabla \cdot \vec{\tau} + \mathbf{g} + \frac{1}{\rho}\mathbf{F}_b \tag{8}$$

where $\mathbf{V}$ is the velocity vector, p is the pressure, τ is the stress tensor, and $\mathbf{F}_b$ represents the body forces per unit volume acting on the fluid. The CSF method [37] is used to model the surface tension as a body force ($\mathbf{F}_b$) that acts only on interfacial cells. The fluid flow is assumed to be Newtonian, laminar, isothermal, and incompressible. The flow Reynolds number for the simulations performed in this study was less than 1.4×10^4, which is far less than the critical Reynolds number (2.57×10^4) reported in the literature for the turbulence inception in the CHJ flows [5].

In the past decade, a number of techniques, each with its own particular advantages and disadvantages, have been developed to

simulate complex multifluid flow problems. Level set methods [38,39] are designed to minimize the numerical diffusion hampering shock-capturing methods and typically define the interface as the zero-level set of a distance function from the interface. The advection of this distance function evolves with the local fluid velocity. A well-known method for tracking the free surface of a liquid is the VOF technique [40], where the computational domain is characterized by a liquid volume fraction function. This function is used to determine both the liquid position and the liquid/gas interface orientation. In this method, a scalar field f (known as volume of fluid fraction) is defined whose value is unity in the liquid phase and zero in the gas. When a cell is partially filled with liquid, i.e., the interface, f will have a value between zero and one

$$f = \begin{cases} 1 & \text{in liquid} \\ >0 \quad <1 & \text{at the liquid-gas interface} \\ 0 & \text{in gas} \end{cases} \tag{9}$$

The discontinuity in f is propagating through the computational domain according to

$$\frac{Df}{Dt} = \frac{\partial f}{\partial t} + \mathbf{V} \cdot \nabla f = 0 \tag{10}$$

For the advection of volume fraction f based on Eq. (10), different methods have been developed. Roughly two important classes of VOF methods can be distinguished with respect to the representation of the interface, namely, simple line interface construction (SLIC) and piecewise linear interface construction (PLIC). Earlier works with VOF were generally based on the SLIC algorithm introduced by Noh and Woodward [41] and the donor-acceptor algorithm published by Hirt and Nichols [42]. The reported literature on the simulation of free-surface flows reveals that the Hirt–Nichols method has been used by many researchers. In this study, however, we used the PLIC method of Youngs [43], which is a more accurate technique. Assuming the initial distribution of f to be given, velocity and pressure are calculated in each time step by the following procedure. The f advection begins by defining an intermediate value of f

$$\tilde{f} = f^n - \delta t \nabla \cdot (\mathbf{V} f^n) \tag{11}$$

Then it is completed with a "divergence correction"

$$f^{n+1} = \tilde{f} + \delta t (\nabla \cdot \mathbf{V}) f^n \tag{12}$$

A single set of equations is solved for both phases; therefore, density and viscosity of the mixture are calculated according to

$$\rho = f\rho_l + (1-f)\rho_g \tag{13}$$

$$\mu = f\mu_l + (1-f)\mu_g \tag{14}$$

where subscripts l and g denote liquid and gas, respectively. New velocity field is calculated according to the two-step time projection method as follows. First, an intermediate velocity is obtained

$$\frac{\tilde{\mathbf{V}} - \mathbf{V}^n}{\delta t} = -\nabla \cdot (\mathbf{V}\mathbf{V})^n + \frac{1}{\rho^n} \nabla \cdot \boldsymbol{\tau}^n + \mathbf{g}^n + \frac{1}{\rho^n} \mathbf{F}_b^n \tag{15}$$

The Poisson equation for pressure is then solved to obtain the pressure field:

$$\nabla \cdot \left[\frac{1}{\rho^n} \nabla p^{n+1} \right] = \frac{\nabla \cdot \tilde{\mathbf{V}}}{\delta t} \tag{16}$$

Next, new time velocities are calculated by considering the pressure field implicitly

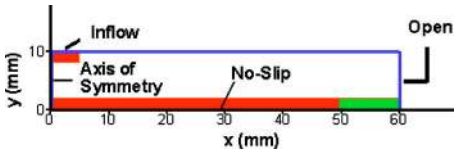

Fig. 4 The flow initial setup along with the specifications of the boundary conditions, the obstacle, and the fluid layer

$$\frac{\mathbf{V}^{n+1} - \tilde{\mathbf{V}}}{\delta t} = -\frac{1}{\rho^n} \nabla p^{n+1} \tag{17}$$

The explicit evaluation of the convective, viscous, and body forces terms in Eq. (15), places restrictions on the magnitude of the allowable time step in order to maintain the stability of the solution. The Poisson equation (Eq. (16)) is solved using an incomplete Cholesky conjugate gradient solver. Further details of the numerical method and Youngs algorithm are given elsewhere [40].

Figure 4 shows the flow initial setup along with the specifications of the boundary conditions applied on the computational domain. As seen in the figure, a small obstacle is added at the end of the domain to preset the flow downstream height. We treat the obstacles as a special case of two phase flow in which the first phase is fluid (liquid and surrounding gas) and the second phase is solid obstacle. The obstacle is characterized as a fluid of infinite density and zero velocity. In general, the obstacle boundaries may snake arbitrarily through the computational mesh. For the simulations in this paper, however, the obstacle boundaries coincide with the lines of the computational grid. The full details of obstacle implementation in the presence of a free surface are given elsewhere [44].

In order to reduce the time of the computation required to reach a steady CHJ, the domain is initially assumed to contain a stagnant fluid layer of the same liquid as of the incoming jet with a thickness equal to that of the obstacle. The boundary conditions for solving the equations, shown in Fig. 4, are as follows. For a solid wall, the no-slip and no-penetration boundary conditions are applied. Also a zero pressure gradient condition is applied across the solid boundaries. For the axis of symmetry—i.e., the left boundary of the computational domain of the CHJ—the velocity of the fluid satisfies the slip and no-penetration conditions, while the gradients of pressure and volume of fluid fraction are zero on the axis of symmetry. The boundary condition used for the right side of the domain is the open boundary, which means the gradients of pressure, volume of fluid fraction, and velocity are all zero. At the top of the computational domain for the inflow boundary, the values of velocity and volume of fluid fraction are set at each time step. The simulations performed in the course of this study were done using an in-house code developed based on the above numerical method and computational procedure.

4 Results and Discussion

The results of simulations for the CHJ based on the VOF method are presented in this section. The location of the jump formation and different characteristics of the CHJ are obtained from the simulations. The effects of various parameters including the downstream height, flow rate, and gravity are also discussed. The simulations are performed for two liquids; tap water and ethylene glycol (EG) and thus the effect of fluid properties is also investigated.

4.1 Mesh Study. Youngs algorithm for free surface advection is more accurate when used in a uniform mesh. In this study, therefore, the grid size was uniform in both directions as shown in Fig. 5 for a sample case. The cell size used in this work was set based on a mesh refinement study in which the grid size was progressively increased until no significant changes were ob-

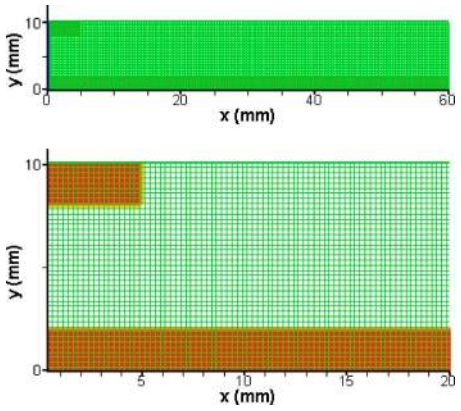

Fig. 5 The computational domain for simulating the CHJ (top) and a magnified view of the uniform grid used for simulation (bottom)

served in the simulation results. The mesh resolution was characterized by a parameter called CPR defined as the number of cells per radius of the incoming jet. Figure 6 shows the jump simulation for different values of CPR for a water jet of 5 mm in radius impacting a solid surface with a flow rate of 30 ml/s and a downstream height of 2 mm. Close inspection of the numerical results showed that for the case with a CPR less than 10, no stable jump was formed leading to a fluctuating jump radius. When the CPR was increased to 15, the jump was stable with a radius of 26.28 mm. Increasing the CPR to 20 slightly changed the jump radius to 26.38 mm. As a result, the jump radius does not change significantly when increasing the CPR value from 15 to 20. For all simulations performed in this study, therefore, a uniform mesh of 20 cells per radius of the jet was used.

4.2 Simulation of Water Circular Jump. The model results are first presented for a base case for which experimental results are available in the literature. The working fluid is tap water with these properties: $\rho=1000$ kg/m^3, $\upsilon=1\times10^{-6}$ m^2/s, and $\sigma=0.073$ N/m. The radius of the incoming jet is $a=5$ mm, the flow rate $Q=30$ ml/s, and the obstacle on the periphery has a height of 2 mm and a length of 10 mm. As explained before (Fig. 4), the obstacle is added to set the downstream height to a desired value. It should be noted that the actual downstream height is usually more than the preset nominal value because the liquid will flow over the obstacle. In order to reduce the computational time needed to reach a stable hydraulic jump, a thin fluid layer with a thickness equal to that of the obstacle is placed on the top of the substrate (see Fig. 4). For the base case with the above conditions, for a typical computational domain of 60×10 mm and a CPR value of 20, the grid size would be 240×40. For such a case, the CPU time was around 1 h on a typical PC with a computational time step of around 10^{-4} s.

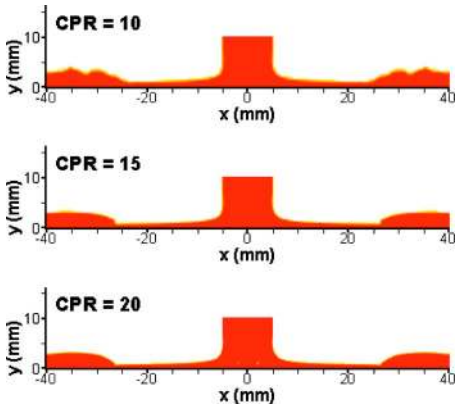

Fig. 6 A mesh study on the CHJ by simulating the jump for different CPR values (for tap water as the working fluid, a flow rate of $Q=30$ ml/s, a jet radius of 5 mm, and a downstream height of $H_\infty=2$ mm)

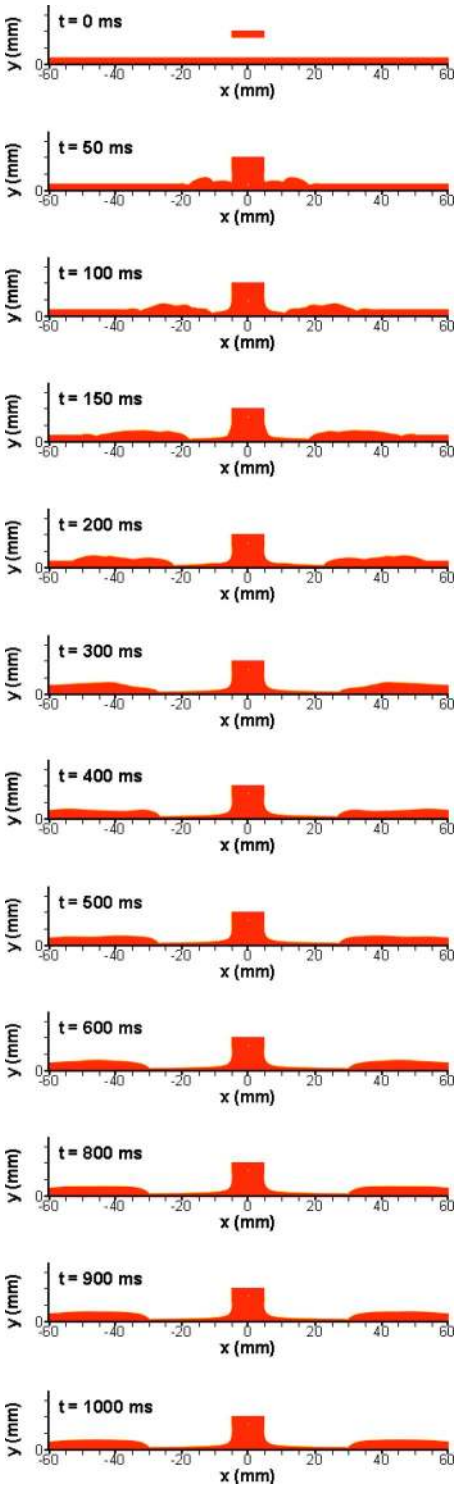

Fig. 7 The evolution of a circular hydraulic jump formation (for tap water as the working fluid, a flow rate of $Q=30$ ml/s, a jet radius of 5 mm, and a downstream height of $H_\infty=2$ mm)

The results of the model for the evolution of a circular hydraulic jump formation for the base case are shown in Fig. 7. From

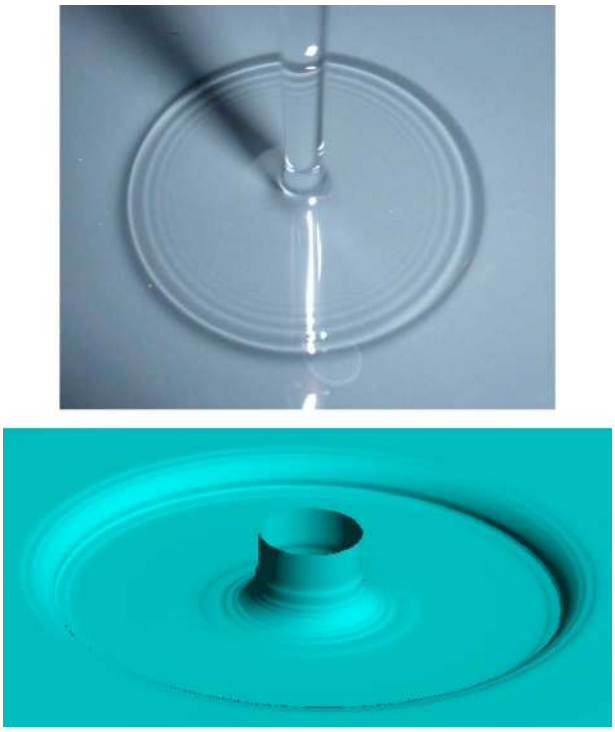

Fig. 8 The 3D view of simulation of the CHJ with a qualitative comparison with experiments [45]

this figure, it is clear that the flow approaches a steady-state condition in less than 1 s elapsed after the introduction of the incoming jet.

A 3D view of the simulated CHJ for the same case as Fig. 7 is compared qualitatively with that of the experiments [45] in Fig. 8. A quantitative comparison of the two results is also performed as presented in Fig. 9 where the variation of the nondimensional jump radius with the Re number is compared with the measurements [13]. As seen in this figure, both results show that the radius of the circular hydraulic jump is increased by increasing the volumetric flow rate (that is increasing the Re number). Close agreement between the predicted jump radius with that of the experiments validates the numerical model and its underlying assumptions.

4.2.1 Effect of Downstream Height and Volumetric Flow Rate. Downstream height or outer depth is one of the most important parameters in the study of circular hydraulic jump and, as seen before (Fig. 3), it is the key parameter in determining the jump

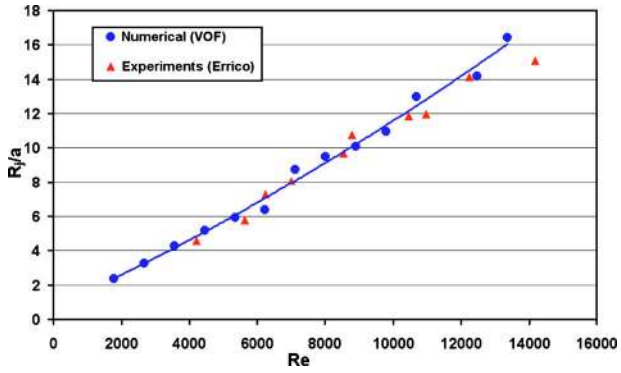

Fig. 9 Comparison of the jump radius from numerical model and experiments (Errico [13])

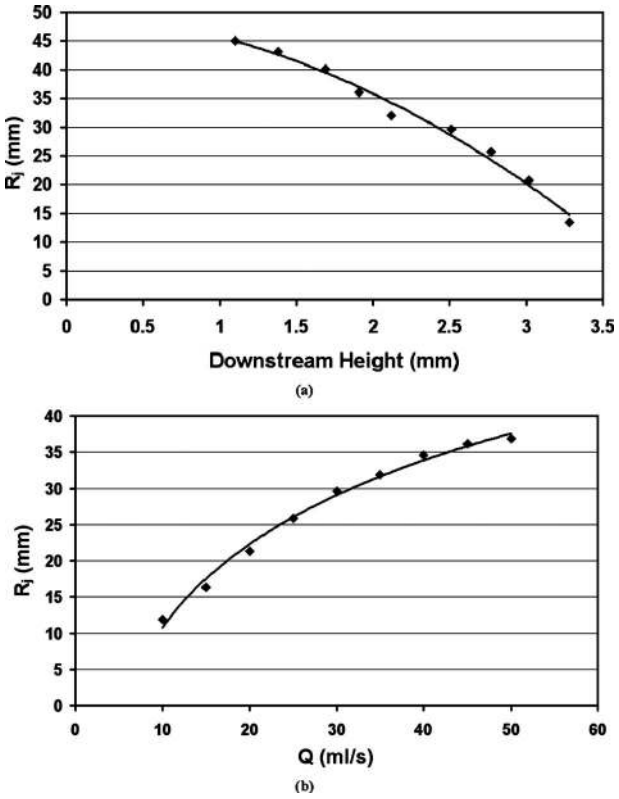

Fig. 10 Variation of jump radius with (*a*) downstream height and (*b*) volumetric flow rate

type. In most experimental works available in the literature, it has been shown that the jump radius is reduced by increasing the downstream height up to a certain limit after which the stability of the jump will be broken and there would be no stable circular hydraulic jump. To investigate the effect of the downstream height in the numerical model, obstacles with a known length and various heights are placed at the end of the computational domain. To reduce the effect of the boundary condition at the periphery of the domain on the jump flow, the appropriate length of the obstacle was found to be 10 mm; this value was obtained based on a large number of simulations performed with different values of the obstacle length. For a value higher than 10 mm, the effect of boundary condition at the periphery vanished. For all simulations in this study, therefore, this value for the obstacle length was used. Figure 10(*a*) shows the effect of the downstream height on the radius of the jump for a 5 mm jet with a flow rate of $Q=30$ ml/s. It is seen quite clearly that the radius of the jump decreases significantly by increasing the downstream height. When the height is increased from 1 mm to 3 mm, the jump radius is decreased by more than 60%. For further increase of the height, no stable jump was observed in the numerical results.

The effect of the volumetric flow rate on the jump radius for a constant jet diameter of 5 mm is given in Fig. 10(*b*). As expected, by increasing the volumetric flow rate, a jump with a larger radius will be formed. An increase of the flow rate from 10 ml/s to 50 ml/s increases the jump radius by 3 times the initial radius.

4.2.2 Effect of Viscosity. It has been verified experimentally, that the liquid viscosity is an important property that has a particular effect on the stability of the CHJ. Water for instance does not always lead to a stable jump because of its low viscosity. That is why Ellegaard et al. [25] had the idea of using a more viscous liquid such as ethylene glycol. Bush and Aristoff [17] also used water-glycerol solution as the working fluid. Using more viscous liquids made it possible to observe and report more stable and

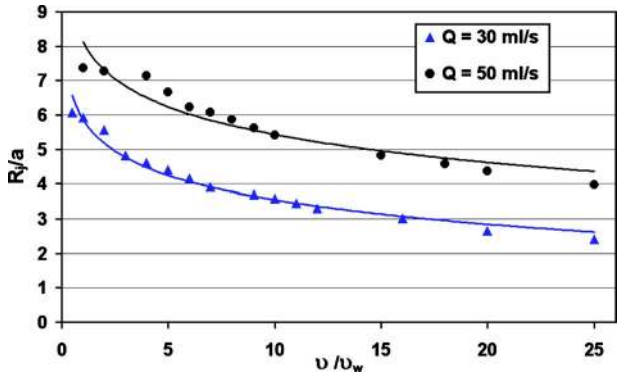

Fig. 11 The variation of circular hydraulic jump radius with viscosity for two different flow rates

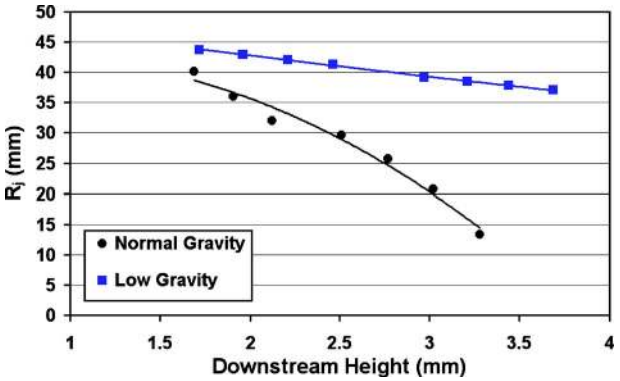

Fig. 13 Comparison between the effect of downstream height on jump radius in normal and microgravity conditions

steady jumps.

The numerical results for variation of jump radius against liquid viscosity, holding other properties constant, for two different flow rates (for a jet radius of 5 mm and an obstacle height of 2 mm) is shown in Fig. 11. The figure is presented in a nondimensional form where the jump radius is scaled by that of the jet, and the viscosity by that of the water (υ_w). When the viscosity increases, the radius of the jump decreases; this is in agreement with the scaling relation of Bohr et al. [21] in which the jump radius is inversely proportional with the viscosity (see Eq. (6)). The figure also reveals a similar behavior of the jump radius to the viscosity variation for different flow rates.

4.2.3 Effect of Gravity. The effect of gravity on circular hydraulic jump was empirically studied in detail by Avedisian and Zhao [1]. In this study, the effect of gravity is investigated numerically; Fig. 12 shows the effect of gravity on the radius of the jump for a jet of radius 5 mm with a flow rate of $Q=30$ ml/s and an obstacle height of 2 mm. The horizontal axis in the figure is the nondimensional gravity ($G=g/g_0$) in which $g_0=9.81$ m/s^2. As seen in the figure, the radius of the jump increases when the gravity is reduced; this is in agreement with what experimentally observed and reported by Avedisian and Zhao [1]. They found that when the gravity decreases, i.e., in low gravity or microgravity conditions, both the radius of the jump and the length of the transition zone increase; thus, the jump occurs more gradually than in normal gravity conditions. The increase of jump radius by decreasing the gravity is also verified by the inviscid theory. As discussed earlier in this paper, based on Watson's derivation for the jump condition (Eq. (1)), the jump radius is inversely proportional to the gravity, i.e., $R_j \propto 1/g$. This behavior is also confirmed by the scaling relation of Bohr et al. (see Eq. (6)).

The microgravity condition also affects the sensitivity of the jump radius variation with respect to the changes in the downstream height. Avedisian and Zhao [1] observed that in low gravity conditions ($G \ll 1$), the radius of the jump is almost independent of the downstream height, i.e., the jump radius is not sensitive to the outer depth as it is in normal gravity conditions. This behavior is also studied numerically here (for $Q=30$ ml/s and a jet of radius 5 mm) and the results are shown in Fig. 13. It should be noted that for low gravity conditions, a value of $G=g/g_0=0.02$ was used for all the simulations, which is the same value used in the experiments by Avedisian and Zhao [1]. As the figure shows, the influence of outer depth on the jump radius in normal gravity is more pronounced than it is in low gravity conditions. This is the same as observed in experiments (see Fig. 16 of Ref. [1]).

The simulations for the effect of gravity are also performed for another case in which the influence of the flow rate on jump radius is studied; the results of these simulations are presented in Fig. 14. As expected, the radius of the jump increases by raising the volumetric flow rate in both normal and low gravity conditions. As expected, however, the jump radius in microgravity is larger than it is in normal gravity. The effect of gravity on the CHJ under various flow rates can be better seen in a cross-sectional view of the jump as shown in Fig. 15 for four different flow rates (for a jet radius of 5 mm and a downstream height of 2 mm). As observed from the figure, in all flow rates, the jump occurs at a larger radius in the low gravity condition. Moreover, the length of the transition zone, i.e., the distance between the upstream and downstream of the jump across which the CHJ occurs, is larger in low gravity than in normal gravity condition. To show the effect of the gravity on gradual occurrence of the jump, a 3D view of the simulations in normal and microgravity conditions is also displayed in Fig. 16.

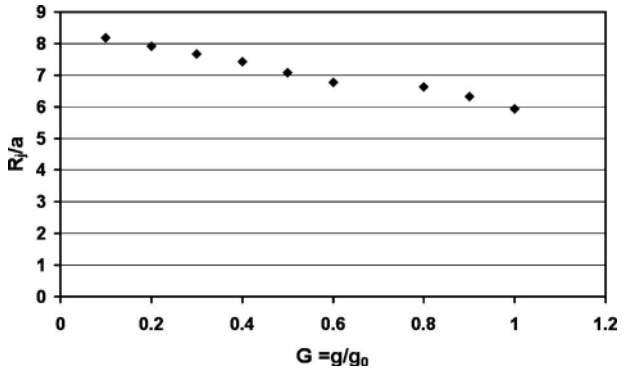

Fig. 12 The variation of jump radius with gravity in a nondimensional form

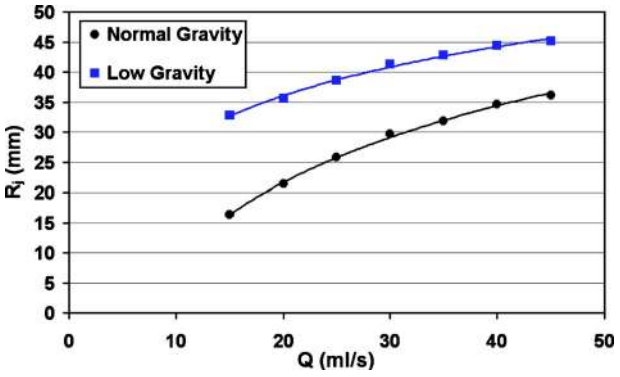

Fig. 14 Comparison between the effect of volumetric flow rate on jump radius in normal and microgravity conditions

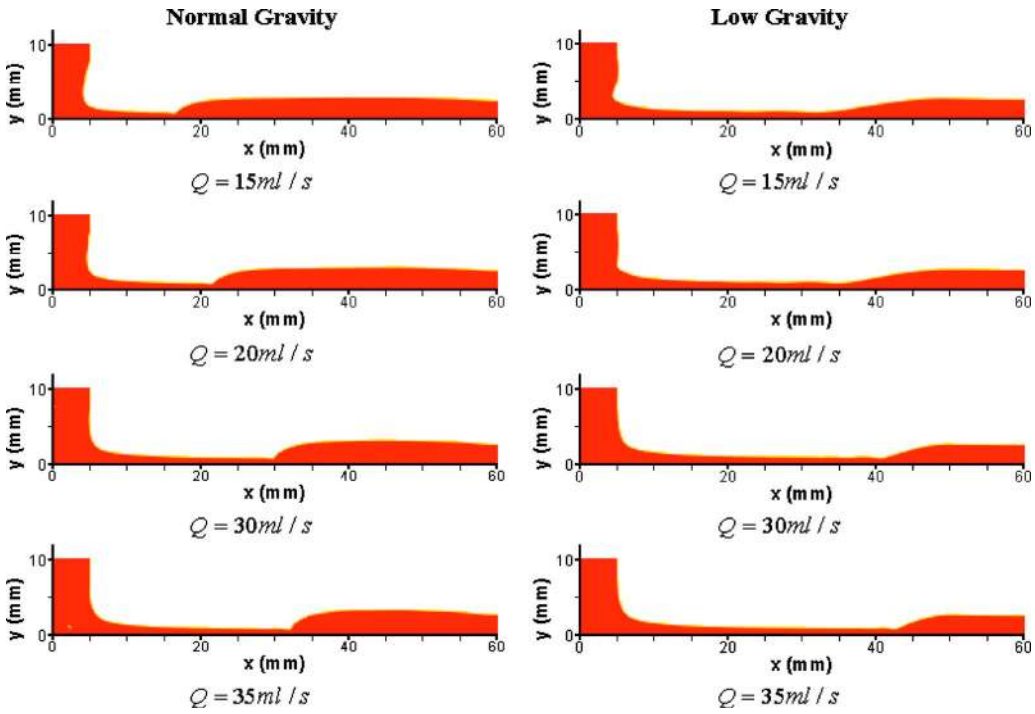

Fig. 15 Circular hydraulic jump in low and normal gravity conditions for four different flow rates

The same observation in experiments has also been reported by Avedisian and Zhao (see Figs. 8 and 9 of Ref. [1]).

4.3 Circular Hydraulic Jump for Ethylene Glycol. In this section, the results of simulations for the formation of the CHJ for another liquid, EG, are presented. As water is not considered a highly viscous fluid, the CHJ for water under certain conditions may not be stable. That is why some investigators chose more viscous liquids such as glycerol-water solution [17] or EG [18,25] in their experiments to study the CHJ.

In Fig. 17 the variations of jump radius with the volumetric flow rate are plotted for a case with EG as the liquid. The figure also shows the results for a water jet with the same conditions. As seen from the figure, the radius of the jump increases when the flow rate is raised for both water and EG. However, the radius of the jump for water is generally larger than that of EG. This is in line with what was discussed earlier that for more viscous liquids there will be smaller jumps (see Fig. 11 and Eq. (6)). The extensive simulations performed in this study reveal that to have a stable CHJ for water, the flow rate cannot exceed a certain limit as seen in Fig. 17. For EG, however, even for large flow rates the obtained CHJ are stable.

The effect of downstream height on jump radius for EG for four different flow rates (for a jet radius of 5 mm) is shown in Fig. 18. As expected, ethylene glycol exhibits the same characteristic as water, i.e., the jump radius decreases with increasing the outer depth and for larger flow rates, there will be bigger jumps. Figure

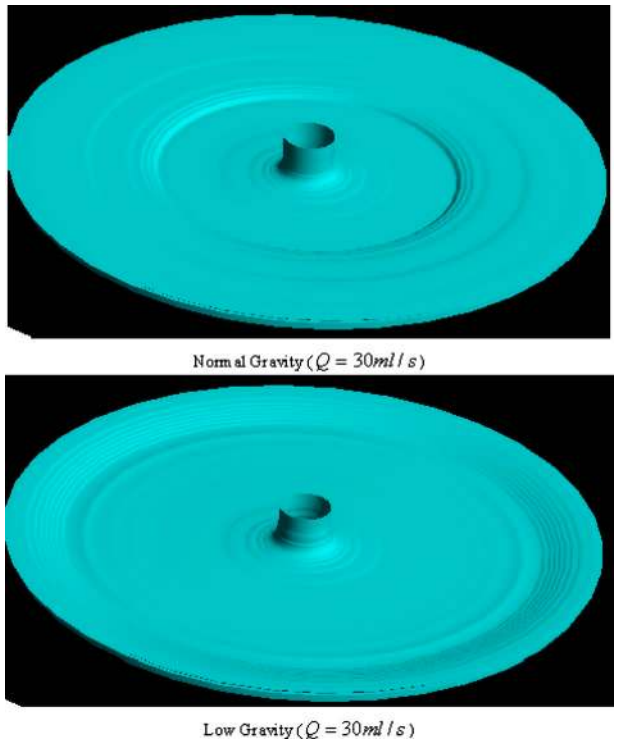

Fig. 16 3D views of circular hydraulic jump in low and normal gravity conditions

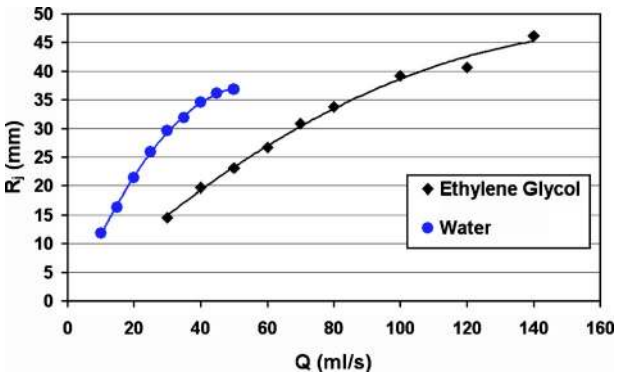

Fig. 17 Comparison of variation of jump radius with flow rate between water and ethylene glycol

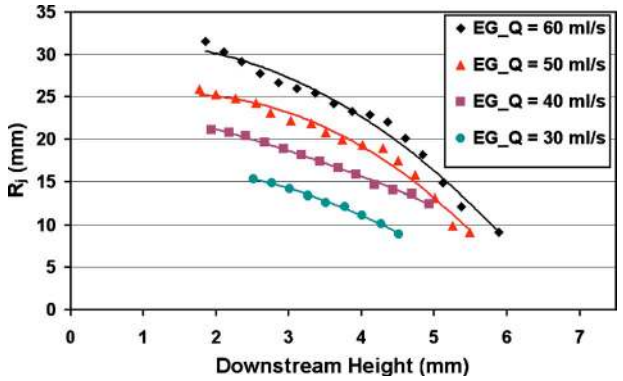

Fig. 18 The effect of downstream height on jump radius for ethylene glycol for different flow rates

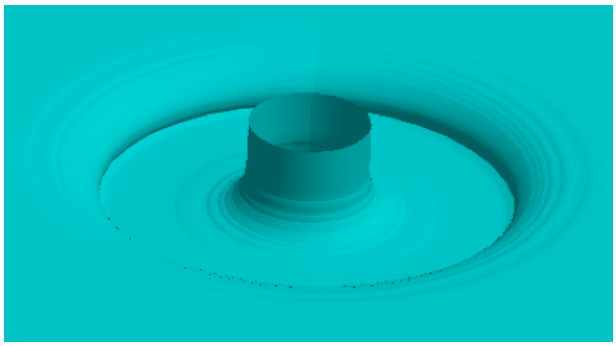

Fig. 20 A 3D view of circular hydraulic jump for ethylene glycol

19 compares the variation of jump radius with the downstream height for both water and EG for $Q=30$ ml/s and a jet radius of 5 mm. It is seen from the figure that the radius of the jump for water is generally larger than that of EG. But more importantly, the figure shows that the sensitivity of jump radius to the downstream height for water is more pronounced. Thus, it can be inferred that for more viscous liquids, the circular hydraulic jump will be less sensitive to the outer depth. The simulations showed that for a water jet with $Q=30$ ml/s, no stable jump was formed for a nominal downstream height of 3 mm and higher. For an ethylene glycol jet with the same flow rate, however, the jump was even formed for a nominal height of 4 mm. This height for larger flow rates, e.g., $Q=60$ ml/s, reaches the value of 5 mm leading to a stable and thick jump. A 3D view of a sample simulation for such a thick jump is presented in Fig. 20 corresponding to a 5 mm EG jet with a flow rate of 50 ml/s and a nominal downstream height of 3.75 mm.

4.4 Types of Circular Hydraulic Jump. From the results presented up to this point, the VOF numerical method was found capable of predicting the CHJ and the effects of various parameters. The model, however, can be used to study different types of the CHJ as discussed earlier in this paper. In Fig. 21, the CHJ for an ethylene glycol jet for $Q=60$ ml/s and a jet radius of 5 mm is presented under different obstacle heights; the flow streamlines surrounding the jump are also shown in the figure. As Fig. 21(*a*) shows for an obstacle height of 1.5 mm, a simple jump with no flow separation (i.e., no vortex) is formed. Increasing the height to 2.5 mm creates a type I jump where a wall vortex is seen on the solid boundary below the free surface right after the jump. When the obstacle height is increased further to a value of 5 mm, both a wall vortex on the solid boundary and a surface roller within the liquid right at the jump location are observed. This jump is called type IIa [18]. For the same height of 5 mm for the obstacle when the flow rate is decreased to 50 ml/s an interesting phenomenon takes place; a double jump also known as type IIb [18] is formed. Figure 22 displays such a case in both 2D and 3D views in which the liquid height is increased twice.

4.5 Comparison With Watson's Theory. A complete quantitative comparison of the model results with those of the theory and experiments is given in this section. The numerical model is run for two liquids of water and EG with various values for jet radius, flow rate and downstream height. The extensive results are then plotted in a nondimensional form as presented in Fig. 23. For the theoretical data, Watson's theory as modified by Bush and Aristoff [17], i.e., Eqs. (4) and (5), are employed. The dashed line seen in the figure is the result of the inviscid theory (Eq. (2)). In

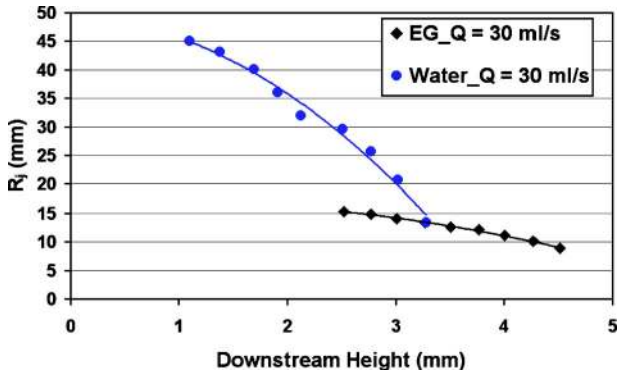

Fig. 19 Comparison of variation of jump radius with downstream height between water and ethylene glycol

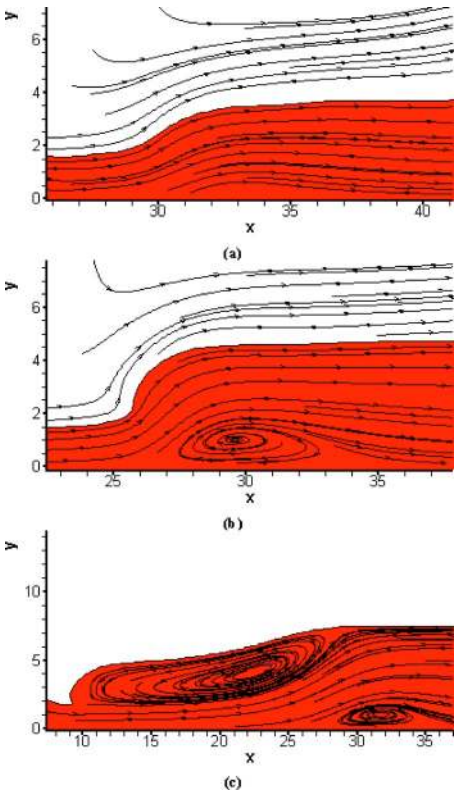

Fig. 21 Different types of circular hydraulic jump obtained from the model: (*a*) jump with no vortex ($H_\infty=1.5$ mm), (*b*) type I jump (with wall vortex) ($H_\infty=2.5$ mm), and (*c*) type IIa jump (with both wall vortex and surface roller) ($H_\infty=5$ mm)

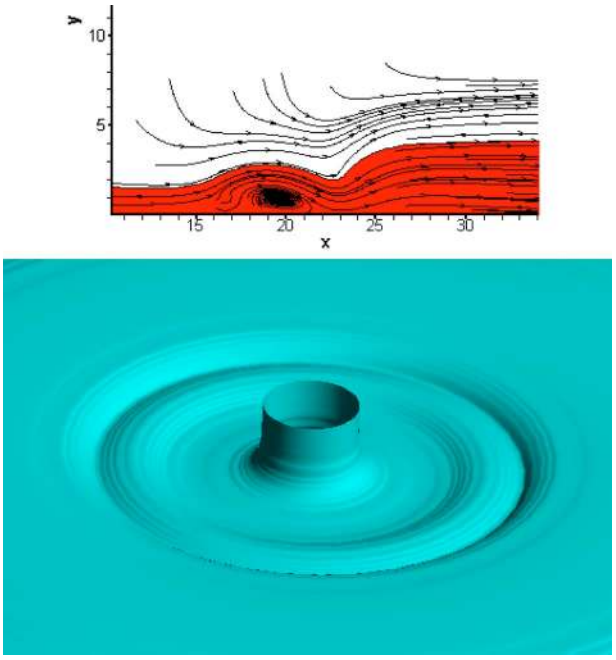

Fig. 22 A 2D and 3D view of the simulation of a double jump

plotting this figure, the same procedure as of Bush and Aristoff [17] has been taken in which the left-hand side of Eqs. (4) and (5) are plotted in terms of a nondimensional term as given in the figure. The figure also contains the experimental results performed by Bush and Aristoff [17]. A close agreement is observed between the predicted values using the VOF numerical model and those of the experiments and theory. From both the simulations and the modified Watson's theory, it can be seen that studying the hydraulic jump without considering the effect of viscosity does not lead to an accurate prediction of the jump location. A close inspection of the numerical results reveals that for ethylene glycol, a better agreement with the theory and experiments compared with that of water is obtained. This comes from the fact that more viscous liquids lead to more stable and steady jumps, as discussed before.

5 Conclusion

In this paper, the impingement of a vertical liquid jet on a solid and horizontal surface, which may lead consequently to the formation of a CHJ, was numerically simulated and the results were compared with those of the theory and experiments. The flow governing equations including the Navier–Stokes equations along with an equation for the advection of the free surface were solved using the volume-of-fluid method. First, the circular hydraulic jump was simulated and compared with experiments. Then the effects of different parameters on the jump radius and its characteristics were studied. The downstream height, volumetric flow rate, viscosity, and gravity were the parameters studied here. The simulations were performed for two different liquids, water and ethylene glycol and they were compared with the modified Watson's theory. The present results agree well with the measurements and the theory; this verified the model and its underlying assumptions. The model was also shown to be capable of simulating the different types of circular hydraulic jump. A brief summary of the numerical results is given below:

- Increasing the flow rate or decreasing the liquid viscosity leads to a larger jump;
- When the downstream height is increased, the radius of the circular hydraulic jump reduces up to a certain limit after which there would be no stable jump;
- If the gravity is decreased, the radius of the jump and the length of the transition zone will both increase, i.e., the circular hydraulic jump is bigger in low gravity than normal gravity conditions;
- The radius of the jump in microgravity conditions is less sensitive to the downstream height than it is in normal gravity;
- For more viscous liquids (e.g., ethylene glycol), the jump is more stable and its location is less sensitive to the downstream height.

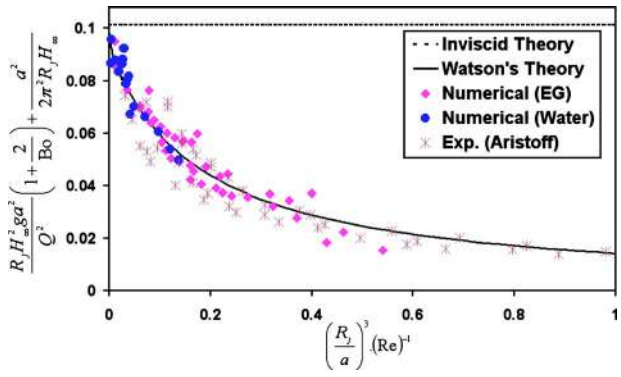

Fig. 23 Comparison of the numerical results with those of the experiments [17] and Watson's theory

Acknowledgment

This work was supported by Research Grant No. 2/15760 from the Ferdowsi University of Mashhad, Mashhad, Iran.

Nomenclature

a = jet radius
Bo = bond number
CHJ = circular hydraulic jump
CPR = cell per radius
f = volume of fluid fraction
$\mathbf{F}_b$ = body force
g = gravitational acceleration
H = upstream height
H_∞ = downstream height
$\mathbf{n}$ = normal unit vector
p = pressure
Q = volumetric flow rate
R_j = jump radius
r_0 = critical radius
Re = Reynolds number
t = time
$\mathbf{t}$ = tangential unit vector
U_0 = incoming jet velocity
$\mathbf{V}$ = velocity vector
VOF = volume-of-fluid

Greek Letters

δ = boundary layer thickness
υ = kinematic viscosity
ρ = density
σ = surface tension
τ = stress tensor

References

[1] Avedisian, C., and Zhao, Z., 2000, "The Circular Hydraulic Jump in Low Gravity," Proc. R. Soc. London, **456**, pp. 2127–2151.
[2] Womac, D. J., Ramadhyani, S., and Incropera, F. P., 1993, "Correlating Equations for Impingement Cooling of Small Heat Sources With Single Circular Liquid Jets," ASME J. Heat Transfer, **115**, pp. 106–115.
[3] Rayleigh, Lord, 1914, "On the Theory of Long Waves and Bores," Proc. R. Soc. London, Ser. A, **90**, pp. 324–328.

[4] Birkhoff, G., and Zarantonello, E., 1957, *Jets, Wakes and Cavities*, Academic, New York.
[5] Watson, E. J., 1964, "The Radial Spread of a Liquid Jet Over a Horizontal Plane," J. Fluid Mech., **20**, pp. 481–499.
[6] Tani, I., 1949, "Water Jump in the Boundary Layer," J. Phys. Soc. Jpn., **4**, pp. 212–215.
[7] Kurihara, M., 1946, "On Hydraulic Jumps," Proceedings of the Report of the Research Institute for Fluid Engineering, Kyusyu Imperial University, **3**(2), pp. 11–33.
[8] Olsson, R., and Turkdogan, E., 1966, "Radial Spread of a Liquid Stream on a Horizontal Plate," Nature (London), **211**, pp. 813–816.
[9] Ishigai, S., Nakanishi, S., Mizuno, M., and Imamura, T., 1977, "Heat Transfer of the Impinging Round Water Jet in the Interference Zone of Film Flow Along the Wall," Bull. JSME, **20**, pp. 85–92.
[10] Nakoryakov, V., Pokusaev, B., and Troyan, E., 1978, "Impingement of an Axisymmetric Liquid Jet on a Barrier," Int. J. Heat Mass Transfer, **21**, pp. 1175–1184.
[11] Bouhadef, M., 1978, "Etalement en Couche Mince d'un Jet Liquide Cylindrique Vertical Saur un Plan Horizontal," Z. Angew. Math. Phys., **29**, pp. 157–167.
[12] Craik, A., Latham, R., Fawkes, M., and Gibbon, P., 1981, "The Circular Hydraulic Jump," J. Fluid Mech., **112**, pp. 347–362.
[13] Errico, M., 1986, "A Study of the Interaction of Liquid Jets with Solid Surfaces," Ph.D. thesis, University of California, San Diego, CA.
[14] Vasista, V., 1989, "Experimental Study of the Hydrodynamics of an Impinging Liquid Jet," B.S. thesis, MIT, Department of Mechanical Engineering.
[15] Liu, X., and Lienhard, J., 1993, "The Hydraulic Jump in Circular Jet Impingement and in Other Thin Liquid Films," Exp. Fluids, **15**, pp. 108–116.
[16] Ellegaard, C., Hansen, A., Haaning, A., Hansen, K., and Bohr, T., 1996, "Experimental Results on Flow Separation and Transition in the Circular Hydraulic Jump," Phys. Scr., **T67**, pp. 105–110.
[17] Bush, J. W. M., and Aristoff, J. M., 2003, "The Influence of Surface Tension on the Circular Hydraulic Jumps," J. Fluid Mech., **489**, pp. 229–238.
[18] Bush, J. W. M., Aristoff, J. M., and Hosoi, A., 2006, "An Experimental Investigation of the Stability of the Circular Hydraulic Jump," J. Fluid Mech., **558**, pp. 33–52.
[19] Bowles, R. I., and Smith, F. T., 1992, "The Standing Hydraulic Jump: Theory, Computations and Comparisons With Experiments," J. Fluid Mech., **242**, pp. 145–168.
[20] Higuera, F. G., 1994, "The Hydraulic Jump in a Viscous Laminar Flow," J. Fluid Mech., **274**, pp. 69–92.
[21] Bohr, T., Dimon, P., and Putkaradze, V., 1993, "Shallow Water Approach to the Circular Hydraulic Jump," J. Fluid Mech., **254**, pp. 635–648.
[22] Bohr, T., Putkaradze, V., and Watanabe, S., 1997, "Averaging Theory for the Structure of Hydraulic Jumps and Separation in Laminar Free Surface Flows," Phys. Rev. Lett., **79**, pp. 1038–1041.
[23] Watanabe, S., Putkaradze, V., and Bohr, T., 2003, "Integral Methods for Shallow Free-Surface Flows With Separation," J. Fluid Mech., **480**, pp. 233–265.
[24] Ellegaard, C., Hansen, A., Haaning, A., Hansen, K., Marcusson, A., Bohr, T., Lundbek Hansen, J., and Watanabe, S., 1998, "Creating Corners in Kitchen Sinks," Nature (London), **392**, pp. 767–768.
[25] Ellegaard, C., Hansen, A., Haaning, A., Hansen, K., Marcusson, A., Bohr, T., Lundbek Hansen, J., and Watanabe, S., 1999, "Polygonal Hydraulic Jumps," Nonlinearity, **12**, pp. 1–7.
[26] Yokoi, K., and Xiao, F., 1999, "A Numerical Study of the Transition in the Circular Hydraulic Jumps," Phys. Lett. A, **257**, pp. 153–157.
[27] Yokoi, K., and Xiao, F., 2002, "Mechanism of Structure Formation in Circular Hydraulic Jumps: Numerical Studies of Strongly Deformed Free-Surface Shallow Flows," Physica D, **161**, pp. 202–219.
[28] Brechet, Y., and Neda, Z., 1999, "On the Circular Hydraulic Jump," Am. J. Phys., **67**(8), pp. 723–731.
[29] Rao, A., and Arakeri, J., 2001, "Wave Structure in the Radial Film Flow With a Circular Hydraulic Jump," Exp. Fluids, **31**, pp. 542–549.
[30] Ferreira, V., Tome, M., Mangiavacchi, N., Castelo, A., Cuminato, J., Fortuna, A., and McKee S., 2002, "High-Order Upwinding and the Hydraulic Jump," Int. J. Numer. Methods Fluids, **39**, pp. 549–583.
[31] Gradeck, M., Kouachi, A., Dani, A., Arnoult, D., and Borean, J., 2006, "Experimental and Numerical Study of the Hydraulic Jump of an Impinging Jet on a Moving Surface," Exp. Therm. Fluid Sci., **30**, pp. 193–201.
[32] Ray, A., and Bhattacharjee, J., 2007, "Standing and Traveling Waves in the Shallow-Water Circular Hydraulic Jump," Phys. Lett. A, **371**, pp. 241–248.
[33] Mikielewicz, J., and Mikielewicz, D., 2008, "A Simple Dissipation Model of Circular Hydraulic Jump," Int. J. Heat Mass Transfer, **52**(1–2), pp. 17–21.
[34] Kate, R., Das, P., and Chakraborty, S., 2008, "An Investigation on Non-Circular Hydraulic Jumps Formed due to Obliquely Impinging Circular Liquid Jets," Exp. Therm. Fluid Sci., **32**, pp. 1429–1439.
[35] Kasimov, A. R., 2008, "A Stationary Circular Hydraulic Jump, the Limits of Its Existence and Its Gasdynamic Analogue," J. Fluid Mech., **601**, pp. 189–198.
[36] Middleman, S., 1995, *Modeling Axisymmetric Flows: Dynamics of Films, Jets and Drops*, Chap. 5, Academic, New York.
[37] Brackbill, J. U., Kothe, D. B., and Zemach, C., 1992, "A Continuum Method for Modeling Surface Tension," J. Comput. Phys., **100**, pp. 335–354.
[38] Sussman, M., and Fatemi, E., 1999, "An Efficient, Interface Preserving Level Set Redistancing Algorithm and Its Application to Interfacial Incompressible Fluid Flow," SIAM J. Sci. Comput. (USA), **20**(4), pp. 1165–1191.
[39] Osher, S., and Fedkiw, R., 2001, "Level Set Methods: An Overview and Some Recent Results," J. Comput. Phys., **169**, pp. 463–502.
[40] Passandideh-Fard, M., and Roohi, E., 2008, "Transient Simulations of Cavitating Flows Using a Modified Volume-of-Fluid (VOF) Technique," Int. J. Comput. Fluid Dyn., **22**(1&2), pp. 97–114.
[41] Noh, W. F., and Woodward, P. R., 1976, "SLIC (Simple Line Interface Construction)," Lect. Notes Phys., **59**, pp. 330–340.
[42] Hirt, F. H., and Nichols, B. D., 1981, "Volume of Fluid (VOF) Method for the Dynamics of Free Boundaries," J. Comput. Phys., **39**, pp. 201–225.
[43] Youngs, D. L., 1982, "Time Dependent Multi Material Flow With Large Fluid Distortion," *Numerical Methods for Fluid Dynamics*, New York Academic Press, New York, pp. 273–285.
[44] Pasandideh-Fard, M., Bussmann, M., Chandra, S., and Mostaghimi, J., 2001, "Simulating Droplet Impact on a Substrate of Arbitrary Shape," Atomization Sprays, **11**, pp. 397–414.
[45] Teymourtash, A. R., Khavari, M., and Passandideh-Fard, M., 2010, "Experimental and Numerical Investigation of Circular Hydraulic Jump," The 18th Annual International Conference on Mechanical Engineering, ISME2010, A. Nouri-Borujerdi and M. R. Movahhedi, eds., Vol. 1, School of Mechanical Engineering, Sharif University of Technology, p. 35, Paper No. 3537.